FOUR-DIMENSIONAL WAVE REFRACTION FROM SENTINEL-1A SATELLITE DATA USING 4-D B-SPLINE ALGORITHM

Maged Marghany

Geoinformation Global Space Technology
130B, Jalan Burhanuddin Helmi,
Taman Tun Dr. Ismail,
60000 Kuala Lumpur
Email:magedupm@hotmail.com

KEY WORDS: 4-D B-spline algorithm, Sentinel-1A data, wave refraction, 4-D wave refraction pattern, Pareto optimization.

ABSTRACT: This study presents a new approach for the simulation of four-dimensional wave refraction pattern in *Sentinel-1A* data. In doing so, the non-linear algorithm exploited to model significant wave height based on the new advance of the 4-D B-spline algorithm. The study shows that wave refraction pattern can simulate from Sentinel-1A data with highest refractive index of 2.6. The study shows that wave refraction pattern can simulate from Sentinel-1A data with convergence and divergence spectra energy. In conclusion, 4-D wave refraction pattern in spite of nonlinearity between actual ocean wave spectra and Sentinel-1A data can be simulated by 4-D B-spline algorithm based on Pareto optimization.

1. INTRODUCTION

At present, there is a great interest for 4-D reconstruction from remote sensing satellite data (Marghany 2014; Marghany 2015). 4-D reconstruction of coastal studies show excellent promises. Marghany and Mansor (2016c) reconstruct 4-D of wave spectra refraction from synthetic Aperture radar (SAR). In fact, SAR wave spectra parameters retrieving are restricted to two ideas that are (i) linear and (ii) nonlinear (Beal et al., 1983, Hasselmann and Hasselmann, 1991, Vachon et al. 1994; Forget and Brochel 1995). These two notions don't seem to be ready to retrieve correct wave spectra parameters. Because the retrieving of wave spectra from SAR is principally influenced by nonlinearity besides the deformation of wave pure mathematics in SAR images owing to shadowing and speckles effects too. There are several efforts to expose on the SAR wave spectra into real wave spectra by exploitation inverse spectra technique as documented on Schulz-Stellenfleth et al., (2007). Further, empirical algorithms are accustomed retrieve deep water vital wave height independent from wave model input. Pleskachevsky et al., (2015), recently implemented the applied math analysis to compared between, input model i.e. CWAM, buoy, and vital wave height was retrieved from TS-X image. However, this procedure involves errors of uncertainty of peak wave amount, the comparative coefficient of dissimilar spectral peaks, and therefore the wind input of the CWAM model. SAR sensors, however, are still not absolutely operational for wave spectra studies.

Shoreline configuration is mainly function of wave refraction. This could be conferred in each convergence and divergence that may cause erosion and deposit, separately. Wave refraction simulation is needed normal algorithms to reconstruct its correct pattern. Consequently, the simulation of wave refection pattern from retrieved wave spectra parameters can expertise with many limitations: (i) ambiguity in direction; (ii) nonlinearity due rate bunching and (iii) the retrieved vital wave height primarily based angle cut-off might be constant through the SAR image. In fact, 2-D FFT may be applied on SAR information with window kernel size of 512 x 512 pixels and features. this implies that the calculable wavelength from 2-DFFT cannot be but 50 m. However, the wave spectra expertise shrinking on their wavelength as they're approaching the shallow water. In this understanding, the simulated SAR image spectrum should be arrayed to be removed from the real wave spectrum and rather sophisticated post-processing is critical for extracting quantitative wave information (Marghany and Mansor 2016c).

The novelty of this work is to optimize the lapses occurring on retrieving wave spectra parameters from SAR information. The most hypotheses is 4-D wave spectra are encoded in 3-D wave spectra as 2-D wave spectra are encoded in 1-D wave spectra. The most objective is to simulate 4-D of wave refraction pattern from Sentinel-1A. this study postulates that (i) 4-D spline able to reconstruct 4-D wave refraction patterns from SAR data and (ii) Pareto optimal solution provide a bet optimization for 4-D wave refraction patterns.

2. DATA ACQUISITION

Two styles of knowledge area unit needed to reconstruct 4-D wave refraction pattern: Sentinel-1 A of SAR; (ii) and therefore the real unaltered wave measuring throughout Sentinel-1 A overpassed.

2.1. Sentinel-1 Data

In this investigation, Sentinel-1 an information with single polarization VV are used. Sentinel-1 (Figure 1) is that the European measuring device Observatory, representing the primary new space part of the GMES (Global observation for setting and Security) satellite family, designed and developed by ESA and funded by the international organization (European Commission). Sentinel-1 consists of a constellation of 2 satellites, Sentinel-1A and Sentinel-1B, sharing a similar orbital plane with a 180° orbital phasing distinction (Figure 2).

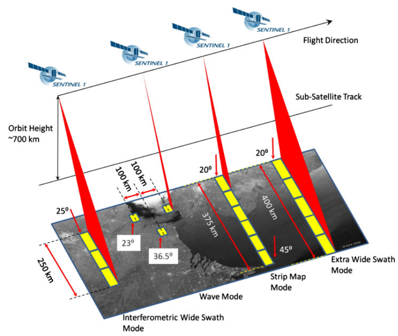

Figure 1. Sentinel-1 A satellite.

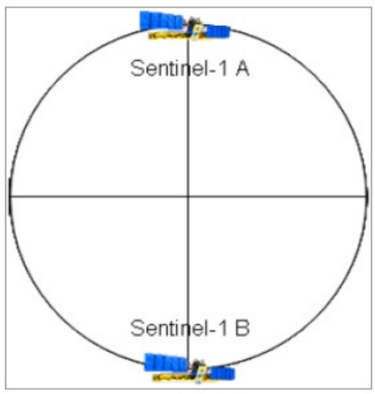

Figure 2. Orbital plane of Sentinel-1A and Sentinel-1B.

Excluding for the ocean wave and current studies, that may be a single polarization mode (HH or VV) with C-band, the SAR instrument should support operations in dual polarization (HH-HV, VV-VH), requiring the implementation of one transmit chain (switchable to H or V) and two parallel receive chains for H and V polarization. The particular wants of the four totally different measure modes with regard to antenna agility need the implementation of an energetic phased array antenna. For every swath the antenna should be designed to come up with a beam with fastened azimuth and elevation inform. Applicable elevation beamforming should be applied for vary ambiguity suppression. Additionally, the incident angle is ranged between 20º-46º (Marghany and Mansor 2016).

2.1 In situ ocean wave measurement

The in situ wave spectra quantities i.e. wavelength, significant wave height, wave period, wave velocity, and direction, are obtained using Acoustic Wave and Current (AWAC) (Figure 3) from the east coast of Kuala Terengganu, Malaysia on March 8th till 12th March 2015, at 5°28'02" N and 103°07'48"E (Figure 3). AWAC recorded the water column current speed and directions.

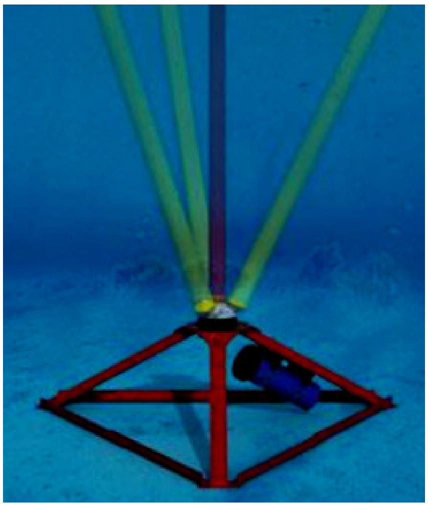

Figure 3. AWAC wave spectra in -situ measurements.

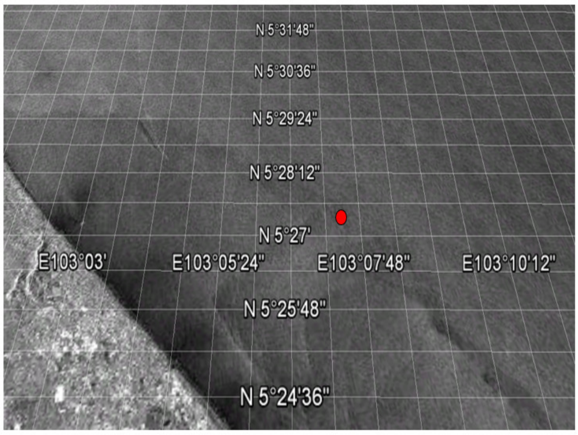

Location of AWAC instrument

Figure 4. Geographical location of AWAC instrument.

3. ALGORITHMS

3.1 4-D Spline Algorithm

Let u, v, and w are constrained to the interval $u, v, w \in [0, 1]$ and $S(u, v, w, t) \in (x, y, z)$. This means that the object is divided into hyperpatches. The hyperpatches are represented using surfaces and curves. Then the surface defined by setting one of u, v, w to a constant integer value which is yelled a knot plane which are the defining the surfaces of hyperpatches (Marghany and Mansor 2016b)Mortenson 1985). The points within the interior and on the boundary of the constant solid is given by (Mortenson 1985). In fact, a volume as a set of 3D area with a further scalar worth given in every of its points. If this scalar worth is taken as a further purpose coordinate, the quantity becomes a 4D "height field" or a hypersurface in 4D area (Marghany and Mansor 2016a). The outlined field are often thought of as a variable of the object's density, temperature, etc. Scalar values are often per the nodes of a daily area grid (voxel data) or by a nonstop operate of 3 variables (so-called implicit surface model or a lot of typically the operate illustration. Albeit traditional thought of area as three-dimensional, any object are often drive within the area of 4 and even higher dimensions. the most challenge is to work out logic strategies to reconstruct such high-dimensional stuffs. This section exploits 4D spline to reconstruct 4-D of Sentinel-1A data.

$$p(u,v,w) = [x\ y\ z] = [x(u,v,w) \quad y((u,v,w) \quad z(u,v,w)] \qquad (1.0)$$

To implement the 4-D spline, the wave spectra parameters which are assimilated at individually knot time and knot planes become temporal functions. Then wave spectra pattern can be expressed in 4D B-spline model as (Amini et al., 1998):

$$S(u,v,w,t)=\sum_{i=1}^{I}\sum_{j=1}^{J}\sum_{k=1}^{K}\sum_{l=1}^{L}E(\vec{K},H_S,t)O_i(u)O_j(v)O_k(w)O_l(t) \qquad (2.0)$$

where O_i (u), O_j (v), O_k (w), and O_l (t) are B-spline basis functions which blend control points of $E(\vec{K},H_S,t)$ and $(I \times J \times K \times L)$ is the total number of model control points. By changing the order of B-spline summation, a more effective method to retrieve a multi-dimensional B-spline wave spectra refraction model results.

3.2 Nonlinear Algorithm

The simplified non-linear theory to record determined Sentinel-1A spectra into the ocean wave spectra which consistent with the Gaussian linear theory, the relation between ocean wave spectra and SAR image spectra might be represented by tilt and hydraulics modulation (real aperture radar (RAR) modulation). The tilt modulation is linear to the native surface slope within the vary direction i.e. within the plane of radiolocation illumination. The tilt modulation generally may be a operate of wind stress and wind direction for ocean waves and Sentinel-1 A. In line with Vachon et al., (1994) the tilt modulation is that the largest for HH polarization. Alpers et al., (1981) and Alpers and Bruning (1986) rumored that hydraulics interaction between the scattering waves (ripples) and longer gravity waves created a degree of the scatterer on the up wind face of the swell. So as to estimate the significant wave height from the quasi-linear remodel, we have a tendency to adopted the algorithmic rule that was given by Marghany (2003) to be acceptable for the geophysical conditions of tropical coastal waters:

$$\lambda_c = \beta\left(\int_{H_{s0}}^{H_{sn}} \sqrt{H_s}\,dH_s + \int_{U_0}^{U_n}\sqrt{U}\,dU\right) \qquad (3.0)$$

where λ_c is cut-off azimuth wavelength, H_s and U are the in situ data of significant wave height and wind speed along the coastal waters of Kuala Terengganu, Malaysia. The measured wind speed was estimated at 10 m height above the sea surface. The changes of significant wave height and wind speed along the azimuth direction are replaced by dH_s and dU, respectively. The subscript zero refers to the average in situ wave data collected before flight pass over by two hours while the subscripts n refers to the average of in situ wave data during flight pass over the study area. β is an empirical value which results of *R/V* multiplied by the intercept of azimuth cut-off (c) when the significant wave height and the wind speed equal zero. A least squares fit was used to find the correlation coefficient between cut-off wavelength and the one calculated directly from the Sentinel-1 A spectra image by equation (1). Then, the following equation was adopted by Marghany (2001) and (2003) to estimate the significant wave height (H_{sT}) from the Sentinel-1 A images

$$H_{sT} = \beta^{-2}\int_{\lambda_{c0}}^{\lambda_{cn}}(\lambda_c)^2\,d\lambda_c. \qquad (4.0)$$

where β is the value of $\left(c\dfrac{R}{V}\right)^{-1}$ and H_{sT} is the significant wave height simulated from Sentinel-1 A images.

The introduced method (azimuthally cut off) is designed for homogeneous wave fields as waves can be found over the open ocean under deep water condition with homogeneous bathymetry. A linear wave transform model can be used to solve the problem of homogeneous wave fields by simulating the physical wave parameters nearshore.

As said by Hasselmann and Hasselmann (1991) and Herbers et al (1999) the wave refraction model over the Sentinel-1A image is developed on the premise of frequency and wave energy conversation principle, mild bathymetry slope, steady wave conditions and solely depth refractive. It are often changed the significant wave height because of refraction into 4-D as follows:

$$E(\vec{K},H_S,t)=S(k_x,k_y,k_z,k_t)\,p(H_S) \qquad (5.0)$$

where $S(k_x, k_y, k_z, k_t)$ is the distribution for the wave number and $p(H_S)$ is the probability distribution of the significant wave height in 4-D.

3.3 Pareto Optimal Solution

Let S [*0,1.....m*] are the wave refraction parameter coefficients that will be estimated by the genetic algorithm to approximate the minimum error for wave refraction parameters. Pareto best solutions are applied to optimize the 4-D wave refraction variation in SAR image. During this drawback, the chromosome consists of variety of genes wherever each gene corresponds to a constant within the nth-order surface fitting polynomial as estimated by

$$f(S_{i,j,k,t}) = S_0 + S_1 i + S_2 j + S_3 k \ + S_4 t + \mathrm{K} + S_m t^n \tag{6.0}$$

where *i,j,k* and *t* are indices of the pixel location in 4-D image respectively, *m* is the number of coefficients. Then the weighted sum to combine multiple objectives into single objective is given by

$$f(S) = w_1 f_1(S) + w_2 f_2(S) + \cdots + w_n f_n(S) \tag{7.0}$$

where $f_1(S), f_2(S), ..., f_n(S)$ are the objective functions and $w_1, w_2, ..., w_n$ are the weights of corresponding objectives that satisfy the following conditions.

$$\begin{aligned} & w_i \geq 0 \quad \forall i = 1,2,...,n \\ & w_1 + w_2 + ... + w_n = 1 \end{aligned} \tag{8.0}$$

Formerly, the weights square measure determined, the looking out direction is fastened. To explore Pareto optimum solutions the maximum amount as attainable, the searching directions ought to be modified once more and once more to sweep over the full resolution space. In this analysis, two objectives are thought of. One is retrieved vital wave height from SAR data and also the alternative is 4-D spline for wave refraction.

4 RESULTS AND DISCUSSION

Figure 5 exposes significant wave height derived by Pareto optimization. The maximum significant wave height is 4.5 m with r2 of 0.8 and RMSE± 0.87m. This agrees with studies of Wrytki, K. (1961); Wong (1981) ; Zelina et al., (2000); Marghany (2004); Marghany (2003) and Marghany et al., (2011). In fact, March is representing northeast monsoon season as wave propagated from the northeast toward the east coast of Malaysia.

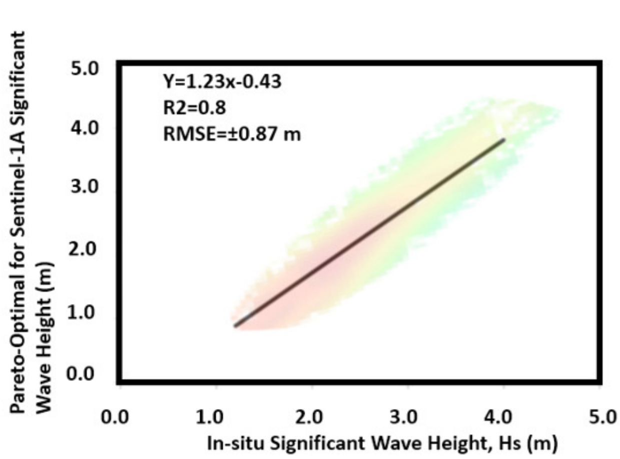

Figure 5. Significant wave height derived from Sentinel-1A image using Pareto optimization.

Figure 6 presents the 4-D wave refraction pattern which derived from 4-D B-spline based Pareto optimal solutions algorithm. 4-D wave refraction pattern shows clear convergence and divergence zone along the coastal water. The divergence zone dominated by breaking significant wave height of 3 m while the convergence zone is dominated by breaking significant wave height of 4.5 m. Moreover, four-dimensional of spectra energy indicates that the convergence zone dominated by highest refractive index of 2.6. In additions, 4-D suggests a turbulent pattern flow which is noticeable by asymmetrical pattern either in convergence or divergence zone (Figur 6).

(a) **(b)**

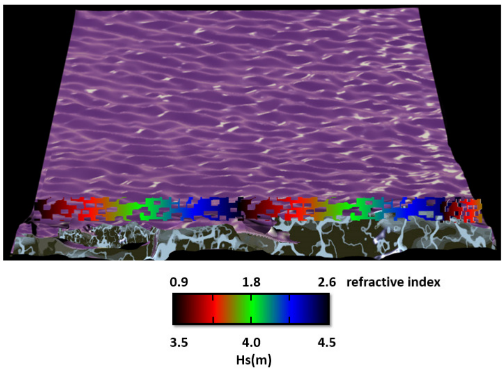

Figure 5. 4-D Wave refraction.

As said by Yudong et al., (2013) and Marghany and Mansor (2016), the energy of 4-D spline is demarcated because the amount of individually knots energy that is pronounced because the integral of the matching apparent that is concluded to the knot plane surface (Waks et al., 1996). All knot planes are optimized though the theoretical operate are fragmented. The 4-D algorithmic rule procedure is all over in the meantime the length is shorter than the edge. Finally, the implementation of Pareto optimum solution improved the 4-D visualization of the wave refraction pattern. Indeed, Pareto-front contains the Pareto-optimal solutions and just in case of continuous front, it divides the target perform space into two components, that are non-optimal solutions and impracticable solutions. With this regard, it amended the strength of pattern search and improved the convergence speed of 4-D B-spline algorithmic rule.

5 CONCLUSION

This study has incontestable a replacement approach for simulation of wave refraction pattern from Sentinel-1A information. In doing therefore, the velocity bunching exploited to model significant wave height supported the new advance of the 4-D B-spline algorithmic program. The study shows that convergence zone is conquered by breaking wave height of 4.5 m The study also indicates that wave refraction pattern can model from Sentinel-1A data with convergence and divergence spectra energy. Lastly, 4-D wave refraction pattern in spite of nonlinearity between actual ocean wave spectra and Sentinel-1A data is simulated by 4-D B-spline algorithmic program supported Pareto optimization.

References

Alpers, W.R., Ross D.B., Rufenach C.L., (1981). On the detectability of ocean surface waves by real and synthetic aperture radar. *Journal of Geophysical Research* 83, 6481-6498.

Alpers, W., and Bruning C., (1986). On the relative importance of motion-related contributions to SAR imaging mechanism of ocean surface waves. *IEEE Transactions on Geoscience and Remote Sensing* 24, 873-885.

Amini, A.A., Y. Chen, R. W. Curwen, V. Mani, and J. Sun, 1998a, Coupled B-Snake Grids and Constrained Thin-Plate Splines for Analysis of 2-D Tissue Deformations from Tagged MRI", IEEE Transactions on Medical Imaging, 17(3):344-356.

Beal., R.C., Tilley, D.G., Monaldo, F.M., (1983). Large-and small-scale spatial evolution of digitally processed ocean wave spectra from seasat synthetic aperture Radar. *Journal of Geophysical Research* 88, 1761-1778.

Forget, F., Broche, P., Cuq, F., (1995). Principles of swell measurement by SAR with application to ERS-1 observations off the Mauritanian coast. *International Journal of Remote Sensing* 16, 2403-2422.

Herbers, T. H. C., S. Elgar and R. T. Guza (1999). Directional spreading of waves in the nearshore, *Journal of Geophysical Research*, **104**, 7683-7693.

Hasselmann, K., Hasselmann S., (1991). On the nonlinear mapping of an ocean spectrum and its inversion". *Journal of Geophysical Research,* **96**, 10,713-10,799.

Li, X., S. Lehner, W. Rosenthal (2010). "Investigation of Ocean Surface Wave Refraction Using TerraSAR-X Data". IEEE Tran. Geos. Rem. Sens. Vol.48,pp.830—840.

Marghany M., (2001). TOPSAR Wave Spectra Model and Coastal Erosion Detection". *International Journal of Applied Earth Observation and Geoinformation*. (3):357-365.

Marghany M., (2003).ERS-1 modulation transfer function impact on shoreline change. *International Journal of Applied Earth Observation and Geoinformation*. (4):279-294.

Marghany M. (2004). "Velocity Bunching Model for Modelling Wave Spectra along East Coast of Malaysia". J. Ind. Soc. Rem. Sens., 32,185-198.

Marghany,M. (2011). Modelling shoreline rate of changes using holographic interferometry. International Journal of the Physical Sciences. Vol. 6(34), pp. 7694 – 7698.

Marghany,M., Mazlan Hashim, and A.P. Cracknell (2011).Simulation of shoreline change using AIRSAR and POLSAR C-band data. Environmental Earth Sciences. 64:1177–1189.

Marghany M.,(2014),"Hologram interferometric SAR and optical data for fourth-dimensional urban slum reconstruction", CD of 35th Asian Conference on Remote Sensing (ACRS 2014), Nay Pyi Taw, Myanmar 27- 31, October 2014,http://www. a-a-r-s.org/acrs/administrator/components/com.../OS-303%20.pdf.[Access on August 2 2016].

Marghany M., (2015), Fourth dimensional optical hologram interferometry of RapidEye for Japan 's tsunami effects" CD of 36th Asian Conference on Remote Sensing (ACRS 2015), Manila, Philippines, 24-28 October 2015, http://www.a-a-r-s.org/acrs/index.php/acrs/acrs-overview/proceedings-1?view=publication&task=show&id=1691, Access on August 2 2016.

Marghany M. and Mansor,S., (2016a). Four-Dimensional Of Sri Lanka Coastal Damages During 2004 Tsunami Using Hologram Interferometry Of Quickbird Satellite Data. CD of 37th Asian Conference on Remote Sensing (ACRS), 37th ACRS from 17th - 21st October 2016, Galadari Hotel, Colombo,Sri Lanka,pp.1-6. http://www.a-a-r-s.org/acrs/index.php/acrs/acrs-overview/proceedings-1?view=publication&task=show&id=2106, Access on September 8 2017.

Marghany M., and Mansor.S. (2016b). Four-Dimensional Phase Unwrapping Algorithm For Retrieving Earthquake Displacement From Sentinel-1a Satellite. CD of 37th Asian Conference on Remote Sensing (ACRS), 37th ACRS from 17th - 21st October 2016, Galadari Hotel, Colombo,Sri Lanka,pp.1-6. http://www.a-a-r-s.org/acrs/index.php/acrs/acrs-overview/proceedings-1?view=publication&task=show&id=2247. Access on September 8 2017.

Marghany,M. and Mansor S. (2016c). Pareto Optimization For Four-Dimensional Wave Refraction Simulation From Sentinel-1A. CD of 37th Asian Conference on Remote Sensing (ACRS), 37th ACRS from 17th - 21st October 2016, Galadari Hotel,Colombo,Sri Lanka,pp.1-6.

Schulz-Stellenfleth, J., König, T., Lehner, S., (2007). An empirical approach for the retrieval of integral ocean wave parameters from synthetic aperture radar data. J. Geophys. Res. 112, C03019.

Pleskachevsky, A., Gebhardt, C., Rosenthal, W., Lehner, S.,Hoffmann, P., Kieser, J., Bruns, T., Lindenthal, A., Jansen, F., Behrens, A., (2015). Satellite-based radar measurements for validation of high-resolution sea state forecast models in the German Bight. Int. Arch. Photogramm. Remote Sens. Spatial Inf. Sci., XL-7/W3 983–990.

Vachon P.W., K.E. Harold and J. Scott. (1994). Airborne and Space-borne Synthetic Aperture Radar Observations of ocean waves. *Journal of Atmospheric.-Ocean* 32 (10) ; 83-112.

Vachon P.W., A. K. Liu and F.C. Jackson (1995). Near-Shore Wave Evolution Observed by Airborne SAR During SWADE. *Journal of Atmospheric.-Ocean* , 2: 363-381.

Vachon, P.W. and J.W.M. Campbell and F.W. Dobson.(1997). Comparison of ERS and Radarsat SARS for Wind and Wave Measurement. *Paper Presented at 3rd ERS Symposium (ESA)* 18-21 March, 1997. Florence, Italy.

Waks, E., Prince, J., Douglas, A (1996). Cardiac Motion Simulator for Tagged MRI. Mathematical Methods in Biomedical Image Analysis , 182–191.

Yudong Z, Shuihua W., Genlin J. and Zhengchao D., (2013). Genetic Pattern Search and Its Application to Brain

Image Classification. Math. Prob. in Eng., 1-8.

Wyrtki,K., (1969). Physical Oceanography of the South-East Asian Waters". *In NAGA Report* Vol. 2, Univ. Calif Scripps Inst. Ocean., La Joll.

Zelina, Z. I., A. Arshad, S.C.Lee, S.B.Japar, A. T. Law, Nik Mustapha, and M. M. Maged, (2000). “East Coast of Peninsular Malaysia”. In: Seas at The Millennium: An Environmental Evaluation. Charles Sheppard (ed.). Elsevier Science LTD London, UK.